# An Experimental and Theoretical Study of Alkali Metal Cation Interactions with Cysteine

**P. B. Armentrout,* Erin I. Armentrout, Amy A. Clark, Theresa E. Cooper, Elana M. S. Stennett, and Damon R. Carl**

*Department of Chemistry, University of Utah, 315 S. 1400 E. Rm 2020, Salt Lake City, Utah*

*Received: November 25, 2009; Revised Manuscript Received: January 27, 2010*

The interactions of alkali metal cations ($M^+ = Li^+$, $Na^+$, $K^+$, $Rb^+$) with the amino acid cysteine (Cys) are examined in detail. Experimentally, bond energies are determined using threshold collision-induced dissociation of the $M^+$(Cys) complexes with xenon in a guided ion beam mass spectrometer. Analyses of the energy dependent cross sections provide 0 K bond energies of 2.65 ± 0.12, 1.83 ± 0.05, 1.25 ± 0.03, and 1.06 ± 0.03 eV for complexes of Cys with $Li^+$, $Na^+$, $K^+$, and $Rb^+$, respectively. All bond energy determinations include consideration of unimolecular decay rates, internal energy of reactant ions, and multiple ion−molecule collisions. Ab initio calculations at the MP2(full)/6-311+G(2d,2p), B3LYP/6-311+G(2d,2p), and B3P86/6-311+G(2d,2p) levels with geometries and zero-point energies calculated at the B3LYP/6-311G(d,p) level for the lighter metals show good agreement with the experimental bond energies. For $Rb^+$(Cys), similar calculations using the HW* basis set and ECP underestimate the experimental bond energies, whereas the Def2TZVP basis set yields results in good agreement. Ground state conformers are tridentate for $Li^+$ and $Na^+$, and subtle changes in the Cys side-chain orientation are found to cause noticeable changes in the alkali metal binding energy. For $K^+$ and $Rb^+$, tridentate and carboxylic acid bound (both charge-solvated and zwitterionic) structures are nearly isoenergetic, with different levels of theory predicting different ground conformers. The combination of this series of experiments and calculations allows the influence of the sulfur functional group of Cys on the overall binding strength to be explored. Comparison to previous results for serine elucidates the influence of sulfur for oxygen substitution.

## Introduction

It is of fundamental interest to quantitatively investigate how the biologically important alkali metal cations interact with amino acids, and by extension how they interact with peptides and proteins. By studying such biologically relevant systems in the gas phase, intrinsic interactions can be quantitatively assessed in the absence of complicating solvent interactions. Such pairwise thermochemical information helps build a "thermodynamic vocabulary"[1] that can be used to enhance our understanding of complicated biological systems. In the present study, we extend previous work on the absolute binding energies of alkali metal cations with amino acids[2−10] to examine $Li^+$, $Na^+$, $K^+$, and $Rb^+$ binding with cysteine (Cys), one of the two common amino acids with sulfur in the side chain (R = $-CH_2SH$). Interactions of metal ions with Cys have direct biological significance but generally involve multiply charged metal cations of Fe, Co, Zn, and Cd.[11−17] A quantitative understanding of the affinity of the sulfur side chain for alkali cations can therefore be useful in examining competition for binding at protein sites involving Cys between these trace metals and the more common alkali cations.

The pairwise interactions of alkali metal cations with the 20 common amino acids have been studied extensively both experimentally and theoretically.[2−10,18−25] Cooks' kinetic method[26,27] has been used to measure the relative cation binding affinities of most of the 20 common amino acids for both lithium[18,19,24] and sodium.[18,23] The average lithium cation binding free energy for Cys at 373 K (determined using Gly and diethoxyethane as references) was reported by Feng et al.[24] as 189 ± 13 kJ/mol, which corresponds to a metal cation binding affinity (enthalpy) of about 230 kJ/mol at room temperature, as calculated using $\Delta S_{373}$ and ($\Delta H_{373} - \Delta H_{298}$) values determined in the present study. For other amino acids, the values from Feng et al. have been found to be systematically low.[5,6,9] For sodium cation affinities, Bojesen et al.[18] found that the value for Cys lay between Ala and Val in their relative measurements. In the more quantitative study of Kish et al.,[23] the sodium cation binding affinity for Cys was found to lie 2.0 kJ/mol above Val and 14.1 kJ/mol above that of Gly. Their absolute affinity scale was anchored to a value for Ala of 167 ± 8 kJ/mol, giving a final 298 K value for $D_{298}(Na^+-Cys)$ of 175 ± 8 kJ/mol. Cysteine is not included among the experimental potassium binding affinities compiled by Tsang and co-workers[28] but is found in the relative binding affinity determinations of $Cu^+$.[29,30] The only previous rubidium binding affinities (experimental or theoretical) come from a recent study that includes Gly, Pro, Ser, and Thr.[10]

These alkali metal cation amino acid complexes have also been studied theoretically.[2−9,20,31−44] These calculations indicate that metal cations bind electrostatically to the functional groups of the amino acid backbone and side chain. Such theoretical predictions have been confirmed by thermodynamic studies involving threshold collision-induced dissociation (TCID) studies of various metalated α-amino acids,[2−9,41] and perhaps more directly by infrared multiple photon dissociation (IRMPD) action spectra of sodiated Gly and proline (Pro),[25] and metalated tryptophan (Trp),[36] arginine (Arg),[37] serine (Ser),[38] threonine (Thr),[39] aspartic and glutamic acid (Asp, Glu),[40] asparagine (Asn),[42] methionine (Met),[43] as well as Cys.[44] In the specific case of cysteine, both sodium and potassium cation complexes have been examined computationally before. Hoyau et al. examined a number of conformations of $Na^+$(Cys) finding a tridentate ground state with a 298 K binding energy of 168 kJ/

10.1021/jp911219u 
Published on Web 02/25/2010

mol calculated at the MP2(full)/6-311+G(2d,2p)//HF/6-31G(d) level of theory including basis set superposition error (BSSE) corrections.[20] These calculations were refined slightly in the work of Kish et al.[23] who report a theoretical sodium cation affinity at 298 K for cysteine of 180 ± 4 kJ/mol calculated at the MP2(full)/6-311+G(2d,2p)//MP2/6-31G(d) level without BSSE corrections. For $K^+$(Cys), Tsang and co-workers[28] determined a theoretical potassium binding affinity of 123.5 kJ/mol at 298 K, calculated at the B3LYP/6-311+G(3df,2p)//B3LYP/6-31G(d) level of theory with zero-point energy corrections taken from HF/6-31G(d) frequency calculations.

The biological significance of pairwise noncovalent interactions indicates that an examination of the metalated Cys systems using a method that can provide absolute thermochemical measurements would be useful. In the present study, the binding affinities of $Li^+$, $Na^+$, $K^+$, and $Rb^+$ with Cys are measured using TCID methods in a guided ion beam tandem mass spectrometer (GIBMS). Complementary quantum chemical calculations are performed for low-lying structures of these complexes and the free ligand at several levels of theory. For completeness, the calculations also include $Cs^+$(Cys) complexes. In addition to providing information necessary for interpretation of the experimental data as well as bond energies for comparison, such calculations allow an examination of how binding energies of the metal cation cysteine complexes vary with conformation. As a multitude of low-energy conformers exist for even simple amino acids, an understanding of the thermodynamic consequences of such conformational changes is useful for better understanding the thermodynamic implications in biological systems. Interestingly, a comparison of metal cation binding to Cys versus Ser[6,38,45] shows more conformational flexibility in the former, such that sulfur for oxygen substitution at the side chain can greatly influence the geometry of metal cation binding sites and as a consequence the relative binding affinities.

## Experimental and Computational Section

**General Experimental Procedure.** The GIBMS used to measure the cross sections for TCID of the alkali metal cation Cys complexes has been described previously in detail.[46,47] Briefly, the ions of interest are formed in either a dc discharge flow tube (DC/FT) source[48] or an electrospray ionization (ESI) source.[49,50] In the DC/FT source, alkali metal ions are generated at the cathode, a tantalum boat filled with the alkali metal located at the head of a 1 m long flow tube, by using a continuous dc discharge with typical operating conditions of 1.9−2.2 kV and 10−20 mA. The alkali metal cations are carried down the flow tube by a buffer gas (ca. 10% argon in helium) with normal operating pressures of 0.3−0.4 Torr. About 50 cm downstream from the discharge, the neutral ligand is introduced into the flow tube using a temperature controlled probe, which is heated to about 180 °C for Cys. Complexes of interest are formed via three-body associative reactions of the alkali cation with Cys in the flow of the He/Ar carrier gas. The complex ions are thermalized to 300 K (the temperature of the flow tube) both vibrationally and rotationally by undergoing ~$10^5$ collisions with the buffer gases as they drift along the 1 m long flow tube.[3,5,48,51−55] In the ESI source, $M^+$(Cys) complexes are formed under conditions similar to those described previously.[50] Briefly, the ESI is operated using a 50:50 by volume $H_2O$/MeOH solution with ~$10^{-4}$ M amino acid and alkali chloride salt (all chemicals purchased from Sigma-Aldrich), which is syringe-pumped at a rate of 0.04 mL/h into a 35 gauge stainless steel needle biased at ~2000 V. In some cases, equimolar amounts of tris(2-carboxyethyl) phosphine were also added to the solution to help stabilize the cysteine. Ionization occurs over the ~5 mm distance from the tip of the needle to the entrance of the capillary, biased at ~35 V. Ions are directed by a capillary heated to 80 °C into a vacuum and a radio frequency (rf) ion funnel,[56] wherein they are focused into a tight beam. Ions exit the ion funnel and enter an rf hexapole ion guide that traps them radially. Here, the ions undergo multiple collisions (>$10^4$) with the ambient gas (largely solvent) and become thermalized to room temperature.[7,50,57]

From either source, the ions are then mass analyzed using a magnetic momentum analyzer, injected into a radio frequency (rf) octopole ion beam guide,[58] where ions are radially trapped and their kinetic energy controlled. The octopole passes through a gas cell that contains Xe at pressures of about 0.05, 0.10, and 0.20 mTorr. To obtain data under rigorously single collision conditions, reaction cross sections are extrapolated to zero reactant pressure prior to threshold analysis.[59] A complete set of pressure measurements was reproduced at least two times for each system. All product and residual reactant ions drift to the end of the octopole where they are extracted, mass analyzed using a quadrupole mass filter, and detected by a 23 kV conversion dynode-secondary electron scintillation detector[60] interfaced with fast pulse counting electronics. The raw ion intensities are converted to cross sections as described elsewhere.[46] The absolute cross sections are estimated to be accurate to ±20% with relative uncertainties of ±5%. Laboratory (lab) collision energies are converted to center-of-mass (CM) energies using the equation $E_{CM} = E_{lab}M/(M + m)$, where $M$ and $m$ are the reactant neutral and ion masses, respectively. All energies cited below are in the CM frame unless otherwise noted. The absolute energy scale and the corresponding full width at half-maximum (fwhm) of the ion beam kinetic energy distribution are determined by using the octopole as a retarding energy analyzer.[46] The energy spread is nearly Gaussian and has a typical fwhm of ~0.3 eV (lab) for the DC/FT source and 0.1−0.2 eV for the ESI source.

**Threshold Analysis.** Analysis of the data to extract threshold energies is achieved by fitting the energy dependent cross sections in the threshold region using eq 1

$$\sigma_j(E) = (N\sigma_0/E)\sum g_i \int_{E_0-E_i}^{E} [1 - e^{-k(E^*)\tau}](E - \varepsilon)^{N-1}\, d(\varepsilon) \quad (1)$$

where $\sigma_0$ is an adjustable energy-independent parameter, $N$ is an adjustable parameter that describes the energy deposition efficiency during collision,[47] $E$ is the relative kinetic energy of the reactants, and $E_0$ represents the CID threshold energy at 0 K. $E_i$ are the internal energies of the rovibrational states $i$ of the reactant ion with populations $g_i$, where $\sum g_i = 1$, such that $E + E_i$ is the total energy available to the colliding reactants. Vibrational frequencies and rotational constants used to calculate $E_i$ and $g_i$ are obtained from the calculations outlined in the next section. The Beyer−Swinehart−Stein−Rabinovitch algorithm[61−63] is used to evaluate the density of the rovibrational states, and the relative populations $g_i$ are calculated for a Maxwell−Boltzmann distribution at 300 K. Equation 1 also includes the effects of unimolecular dissociation kinetics during the time available for dissociation, $\tau$ ~$5 \times 10^{-4}$ s.[47] The kinetics are estimated using the Rice−Ramsperger−Kassel−Marcus (RRKM) theory,[64−66] as described in detail elsewhere,[67,68] where $\varepsilon$ is the energy transferred from translation into internal energy of the complex during the collision and $E^*$ is the internal energy of the energized molecule (EM), i.e., $E^* = \varepsilon + E_i$. The term $k(E^*)$

is the unimolecular rate constant for dissociation of the EM, as defined by RRKM theory in eq 2

$$k(E^*) = dN^{\dagger}_{vr}(E^* - E_0)/h\rho_{vr}(E^*) \quad (2)$$

where $d$ is the reaction degeneracy, $h$ is Planck's constant, $N^{\dagger}_{vr}(E^* - E_0)$ is the sum of rovibrational states of the transition state (TS) at an energy $E^* - E_0$, and $\rho_{vr}(E^*)$ is the density of rovibrational states of the EM at the available energy, $E^*$. To evaluate the rate constant in eq 2, vibrational frequencies and rotational constants for the EM and TS are required. Because the metal−ligand interactions in the complexes studied here are mainly long-range electrostatic interactions (ion−dipole, ion−quadrupole, and ion−induced dipole interactions), the most appropriate model for the TS for $M^+$(Cys) complexes dissociating to $M^+$ + Cys is a loose association of the ion and neutral ligand,[2,3,53,69−71] even for multidentate ligands.[57,72−74] Therefore, the TSs are treated as product-like, such that the TS frequencies are those of the dissociated products. The transitional frequencies are treated as rotors, a treatment that corresponds to a phase space limit (PSL), as described in detail elsewhere.[67,68] The three transitional mode rotors have rotational constants equal to those of the ligand product. The 2-D external rotations are treated adiabatically but with centrifugal effects included.[75] In the present work, the adiabatic 2-D rotational energy is treated using a statistical distribution with an explicit summation over all possible values of the rotational quantum number.[67]

When compared to the experimental data, the cross section calculated using eq 1 is convoluted over the kinetic energy distribution of the ion beam and thermal energy distribution of the neutral collision gas (Doppler broadening), as described elsewhere.[46] Uncertainties in the fitting parameters are obtained from variations associated with different data sets, the parameter $N$, changes in the vibrational frequencies (±10% for most vibrations and a factor of 2 for the $M^+$−Cys modes), variations in $\tau$ by a factor of 2, and the uncertainty in the absolute energy scale, ±0.05 eV (lab).

In deriving the final optimized bond energies at 0 K, two assumptions are made. First, there is no activation barrier in excess of the endothermicity for the loss of ligands, which is generally true for ion−molecule reactions, especially the heterolytic noncovalent bond cleavages considered here.[76] Second, the measured threshold is assumed to correspond to dissociation of the ground state reactant to ground state ion and neutral ligand products. Given the relatively long experimental time frame available (~$5 \times 10^{-4}$ s) for the energized complexes to explore phase space, we assume that the dissociating complexes are able to rearrange to their ground state product conformations upon dissociation. The appropriateness of this assumption for the Cys ligand is nicely verified by the good agreement between our experimental results with theoretical values, as discussed below.

**Computational Details.** Our protocol for finding all low-lying conformations of metal cation−amino acid complexes has been described elsewhere.[2,3,5−10] Final geometry optimizations and frequency calculations use density functional theory (DFT) at the B3LYP/6-311G(d,p) level,[77,78] which has been shown to be adequate for accurate structural descriptions of comparable metal cation−ligand systems.[2−10] Zero-point vibrational energy (ZPE) corrections were determined using these vibrational frequencies after scaling by 0.9804.[79] Single point energy calculations were carried out for the lowest 22−24 optimized structures at the B3LYP, B3P86, and MP2(full) levels using the 6-311+G(2d,2p) basis set. Basis set superposition errors (BSSEs) in all bond dissociation energy calculations were estimated using the full counterpoise (cp) method.[80,81] Previous work[2,3,71,82,83] has indicated that BSSE corrections on alkali metal systems are generally small for DFT calculations, and we find this to be true here as well. Both B3LYP and B3P86 calculations have BSSE corrections of 1−4 kJ/mol, whereas the MP2(full) values have BSSE corrections of 4−12 kJ/mol.

A comprehensive analysis of lithium cation affinities reveals that core electron correlation on the lithium cation is needed to better describe the interaction energy of lithium with a variety of ligands.[84] Therefore, we also optimized the ground state structures of $Li^+$(Cys) systems at the MP2(full) level of theory using the cc-pCVDZ basis set for $Li^+$ and cc-pVDZ basis set for other atoms, designated as cc-pVDZ(Li−C) below. Single point energies were calculated using B3LYP, B3P86, and MP2(full) levels with the cc-pCVTZ for $Li^+$ and aug-cc-pVTZ basis sets for other atoms, designated as aug-cc-pVTZ(Li−C) below. No counterpoise corrections are made to these single point energies, as these have been shown to reduce the accuracy of the MP2 computational results.[84]

For complexes of the heavier metal cations, $Rb^+$ and $Cs^+$, all conformations found for $K^+$(Cys) were used as starting points for geometry and vibrational frequency calculations optimized at the B3LYP/HW*/6-311G(d,p) level, where HW* indicates that $Rb^+$ and $Cs^+$ were described using the effective core potentials (ECPs) and valence basis sets of Hay and Wadt[85] with a single d polarization function (exponents of 0.24 and 0.19, respectively) added.[86] Relative energies are determined using single point energies at the B3LYP, B3P86, and MP2(full) levels using the HW*/6-311+G(2d,2p) basis set. Previous work on analogous complexes of serine suggests that the use of the HW* basis sets for the $Rb^+$ and $Cs^+$ systems should yield equivalent results to the all-electron basis sets used for the smaller cations.[38] For the three lowest energy conformers found for $Rb^+$ complexes, we also performed geometry optimizations and frequency calculations at the B3LYP/Def2TZVP level followed by single point energy calculations at the B3P86/Def2TZVP and MP2(full)/Def2TZVP levels. The Def2TZVP basis sets are of triple-$\zeta$ valence quality plus polarization for all elements,[87] and use a small core 28 electron ECP developed by Leininger et al. for Rb.[88]

## Results

**Cross Sections for Collision-Induced Dissociation.** Experimental cross sections were obtained for the interaction of Xe with $M^+$(Cys), where $M^+ = Li^+$, $Na^+$, $K^+$, and $Rb^+$, as a function of collision energy. Figure 1 shows representative data extrapolated to zero pressure of Xe for collision-induced dissociation (CID) of the three heavier metal complexes. Detailed results for $Li^+$(Cys) are provided in a companion paper (DOI 10.1021/jp911222j) because of the complexity of the data and its analysis.[89] Over the energy ranges examined, the loss of the intact amino acid, reaction 3, is seen in all four $M^+$(Cys) systems, and this is the only dissociation channel observed for $Na^+$−$Rb^+$.

$$M^+(Cys) + Xe \rightarrow M^+ + Cys + Xe \quad (3)$$

The relative thresholds of the cross sections for this process decrease from $Li^+$ to $Na^+$ to $K^+$ to $Rb^+$, reflecting the decrease in the binding energy to the intact amino acid. This is consistent with previous threshold CID bond dissociation energy measurements of metallized amino acids[1−4,9,10] and many other ligands.[90]

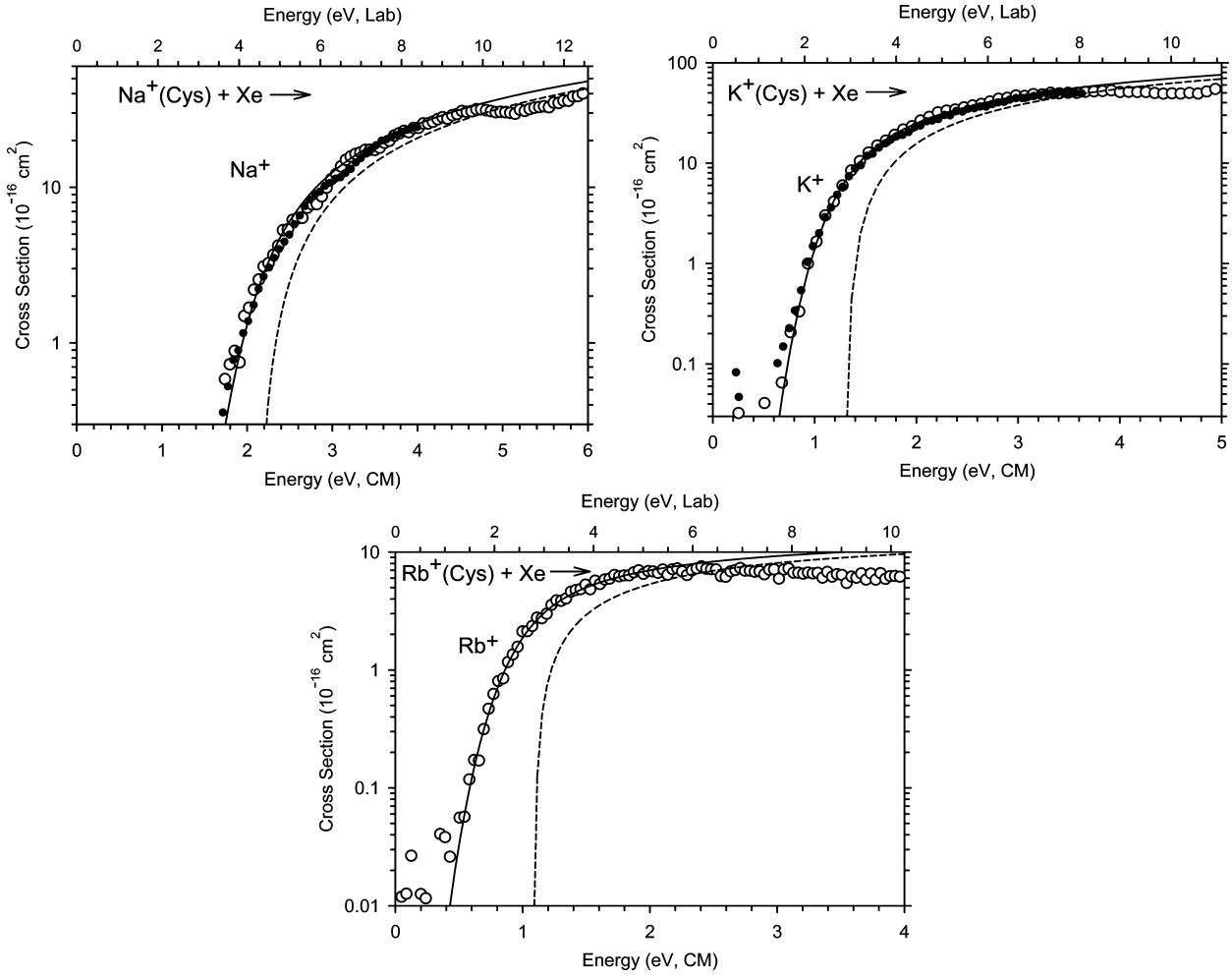


**Figure 1.** Zero pressure extrapolated cross sections for collision-induced dissociation of $Na^+$(Cys), $K^+$(Cys), and $Rb^+$(Cys) with xenon as a function of kinetic energy in the center-of-mass frame (lower *x*-axis) and the laboratory frame (upper *x*-axis). Closed and open (scaled up by factors of 4 and 8 for $Na^+$(Cys) and $K^+$(Cys), respectively) symbols show data taken using the flow tube and electrospray ion sources, respectively. Solid lines show the best fit to the data using the model of eq 1 convoluted over the neutral and ion kinetic and internal energy distributions. Dashed lines show the model cross sections in the absence of experimental kinetic broadening for reactants with an internal energy of 0 K.

**TABLE 1: Fitting Parameters of eqs 1 and 2, Threshold Dissociation Energies at 0 K, and Entropies of Activation at 1000 K for CID of $M^+$(Cys) with Xe[a]**

| reactant | source | products | $\sigma_0$ | $N$ | $E_0$[b] (eV) | $E_0$(PSL) (eV) | $\Delta S^{\ddagger}_{1000}$ (J/mol K) |
|---|---|---|---|---|---|---|---|
| $Li^+$(Cys)[c] | FT | $Li^+$ + Cys | 9.7 (2.9) | 1.1 (0.2) | | 2.65 (0.12) | 50 (2) |
| $Na^+$(Cys) | ESI | $Na^+$ + Cys | 2.7 (0.2) | 1.8 (0.1) | 2.08 (0.18) | 1.83 (0.06) | 44 (2) |
| | FT | $Na^+$ + Cys | 27.7 (7.8) | 1.6 (0.3) | 2.06 (0.14) | 1.86 (0.14) | 44 (2) |
| $K^+$(Cys) | ESI | $K^+$ + Cys | 8.2 (0.8) | 1.4 (0.1) | 1.34 (0.04) | 1.26 (0.04) | 38 (22) |
| | FT | $K^+$ + Cys | 46.0 (5.0) | 1.5 (0.1) | 1.32 (0.05) | 1.23 (0.05) | 38 (22) |
| $Rb^+$(Cys) | ESI | $Rb^+$ + Cys | 13.6 (3.7) | 1.1 (0.1) | 1.11 (0.03) | 1.06 (0.03) | 18 (10) |

[a] Uncertainties are listed in parentheses. [b] Does not include lifetime effects. [c] Competitive fitting results from the companion paper (DOI 10.1021/jp911222j).[89]

In the $Na^+$ and $K^+$ systems, data is available for ions generated using both the ESI and DC/FT sources. The absolute magnitudes of the cross sections obtained for the two sources do not agree particularly well (with the ESI source yielding cross sections that are smaller by factors of 4 and 8, respectively), for reasons that are not understood. Despite this difference, the energy dependences in both systems are clearly identical within experimental uncertainty. This demonstrates that both sources have adequately thermalized the cationic complexes to consistent temperatures of 300 K and that the differences in magnitudes cannot be a result of a drastically different distribution of conformations.

**Threshold Analysis and Results.** Cysteine losses in reaction 3 were modeled using eq 1. Figure 1 shows that the experimental cross sections are reproduced well by eq 1 over extended energy and magnitude ranges. The optimized parameters of eq 1 for all systems using molecular parameters for the ground state complexes and PSL transition states calculated at the B3LYP/6-311+G(d) level (see next section) are reported in Table 1, with values for $Li^+$(Cys) taken from a more complicated analysis that includes competition with other lower energy decomposition channels, as detailed in a companion paper (DOI 10.1021/jp911222j).[89] The difference between threshold values with and without RRKM lifetime analysis equals the kinetic shift for $M^+$(Cys): 0.80,[89] 0.25, 0.08, and 0.04 eV for $Li^+$, $Na^+$, $K^+$, and $Rb^+$, respectively. These are slightly higher than for the analogous complexes of Ser,[6] which has the same size side chain, and smaller than those of the complexes of Thr,[6] which

**TABLE 2: B3LYP, B3P86, and MP2(full) 0 K Relative Energies (kJ/mol) of Low-Lying Conformers of $M^+$(Cys)[a]**

| structure | dihedrals[b] | $Li^+$(Cys) | $Na^+$(Cys) | $K^+$(Cys) | $Rb^+$(Cys)[c] | $Cs^+$(Cys) |
|---|---|---|---|---|---|---|
| [N,CO,S] | $tggg_+$ | **0.0**, **0.0**, **0.0** | **0.0**, **0.0**, **0.0** (**0.0**)[d] | **0.0**, 0.8, **0.0** | 2.4, 4.7, **0.0**<br>*0.4*, *3.4*, ***0.0*** | 7.1, 9.5, 0.8 |
| | $tggg_-$ | 2.8, 3.0, 3.4 | 4.6, 3.4, 4.1 | 4.9, 4.4, 5.0 | 6.2, 8.8, 5.3<br>*3.3*, *6.5*, *5.7* | 11.0, 13.7, 5.9 |
| [COOH] | $ctg_-g_-$ | 54.9, 51.1, 59.4 | 26.8, 22.6, 27.8 | 6.3, 4.5, 10.8 | **0.0**, **0.0**, 3.4<br>***0.0***, *0.3*, *5.6* | 0.6, 0.7, 0.8 |
| | $ctg_-g_+$ | 55.4, 51.0, 59.8 | 27.4, 22.7, 28.2 | 7.0, 5.1, 11.3 | 0.5, 0.02, 3.2<br>*0.1*, ***0.0***, *5.1* | **0.0**, **0.0**, **0.0** |
| | cgtg | 56.2, 52.2, 65.8 | 31.4, 26.9, 34.0 | 11.0, 9.7, 17.1 | 4.4, 4.2, 8.8<br>*3.8*, *4.1*, *11.1* | 3.6, 4.0, 6.3 |
| | cttg | 59.7, 56.5, 70.3 | 35.0, 31.5, 38.6 | 14.2, 13.9, 21.7 | 7.8, 8.5, 13.8 | 7.2, 8.4, 10.7 |
| | cgtt | 63.8, 59.9, 70.3 | 35.7, 31.6, 38.6 | 15.4, 14.5, 22.3 | 8.8, 9.1, 14.1 | 7.3, 7.9, 10.7 |
| | $ctg_+g_-$ | 69.5, 66.3, 76.3 | 41.5, 37.9, 44.7 | 20.7, 20.4, 27.6 | 13.9, 14.5, 19.1 | 13.6, 14.7, 15.8 |
| [$CO_2^-$] | $ctg_-g_+$ | 22.4, 19.6, 24.2 | 10.9, 7.0, 11.0 (11.3)[d] | 3.3, **0.0**, 7.1 | 5.0, 3.0, 7.9<br>*3.6*, *2.2*, *6.3* | 10.4, 7.8, 9.7 |
| | cgtg | 25.4, 23.8, 29.4 | 14.3, 11.7, 16.8 | 6.8, 4.8, 13.1 | 9.0, 8.3, 14.2 | 14.5, 13.4, 16.4 |
| | $ctg_-g_-$ | 26.4, 23.5, 29.6 | 14.8, 10.9, 16.5 | 6.8, 3.6, 12.2 | 8.8, 6.9, 13.2 | 14.5, 11.9, 15.4 |
| | cgtt | 29.9, 28.3, 34.3 | 18.6, 16.0, 21.4 | 11.2, 9.3, 17.9 | 13.2, 12.6, 18.7 | 18.7, 17.6, 21.2 |
| | $ctg_+g_-$ | 47.5, 46.8. 51.6 | 34.7, 32.5, 36.9 | 25.6, 23.7, 31.7 | 26.0, 25.1, 30.7 | 30.6, 28.8, 31.9 |
| [N,CO] | $tcgg_+$ | 16.5, 17.0, 20.8 | 15.0, 14.2, 16.0 | 9.2, 9.6, 12.1 | 9.4, 11.4, 10.0 | 12.0, 14.3, 9.4 |
| | tgtg | 18.8, 19.6, 25.0 | 17.9, 16.0, 19.5 | 11.5, 11.3, 15.0 | 10.2, 12.6, 12.4 | 12.8, 15.5, 11.4 |
| | $tcgg_-$ | 19.0, 19.6, 24.2 | 19.2, 17.2, 19.6 | 13.6, 12.7, 15.8 | 12.0, 14.3, 13.4 | 14.6, 17.3, 12.8 |
| | $tctg_-$ | 23.9, 25.4, 30.9 | 23.0, 21.5, 25.5 | 15.1, 16.7, 20.6 | 14.0, 16.5, 17.3 | 16.3, 19.1, 16.2 |
| | tgtt | 24.3, 25.3, 30.8 | 23.8, 22.2, 25.7 | 16.9, 18.7, 21.5 | 16.6, 19.2, 19.2 | 19.5, 22.4, 18.4 |
| | $tctg_+$ | 26.9, 28.4, 34.6 | 24.5, 24.7, 28.8 | 17.6, 19.0, 24.0 | 16.7, 19.6, 20.6 | 20.0, 22.6, 20.0 |
| | tctt | [N,CO] tgtt | 28.6, 27.1, 30.4 (31.8)[d] | [N,CO] $tctg_-$ | [N,CO] $tctg_-$ | [N,CO] $tctg_-$ |
| [CO,S] | ctgt | 31.9, 30.4, 43.7 | 24.9, 21.4, 31.6 | 11.6, 11.3, 19.3 | 8.5, 8.1, 14.2 | 9.3, 9.1, 11.2 |
| | ctcg | 46.0, 44.4, 57.8 | 33.0, 30.0, 39.0 (41.8)[d] | [COOH] $ctg_-g_-$ | [COOH] $ctg_-g_-$ | [COOH] $ctg_-g_-$ |
| | ttgt | 48.8, 49.7, 58.2 | 40.6, 40.4, 45.4 (49.4)[d] | 29.7, 30.9, 33.8 | 24.1, 28.4, 28.2 | 24.9, 29.3, 24.7 |
| [N,OH,S] | $tggg_+$ | 32.2, 33.9, 29.0 | 30.1, 31.4, 26.8 (27.2)[d] | 28.3, 30.0 25.4 | 28.7, 31.7, 23.4 | 33.0, 35.5, 24.2 |
| | $tggg_-$ | 34.2, 37.2, 32.8 | 34.6, 36.5, 33.1 | 33.9, 36.1, 33.1 | 35.4, 38.6, 31.4 | 40.0, 42.7, 32.0 |

[a] B3LYP, B3P86, and MP2(full) values calculated using the 6-311+G(2d,2p) basis sets with structures and zero-point energies calculated at the B3LYP/6-311G(d,p) level of theory. Values for Rb and Cs use the HW* basis set on the metal. Bold indicates the ground state. Entries having alternate structures indicate the calculation collapsed to the indicated structure. [b] Dihedral angles for ∠HOCC, ∠OCCC, ∠CCCS, and ∠CCSH. [c] Values in italics calculated using the Def2TZVP basis set. [d] MP2/6-31G*//HF/6-31G* values from Hoyau et al.[20]

has a longer side chain. Thus, the size of the kinetic shift varies such that higher $E_0$ values and more complicated ligands yield larger kinetic shifts. The relatively large kinetic shift values found here indicate the importance of incorporating RRKM theory into the threshold analysis when dealing with such complex systems.

Table 1 also includes $\Delta S^{\ddagger}_{1000}$ values, which reflect the looseness of the transition states. In all cases, the $\Delta S^{\ddagger}$ values for losing intact ligands are 18−50 J/mol·K, which is consistent with the assumption of loose transition states for the $M^+$(Cys) systems.

**Theory: Cysteine.** As described above, low-energy structures of neutral Cys were optimized at the B3LYP/6-311G(d,p) level of theory. Relative single point energies, which include zero-point energy (ZPE) corrections, are calculated at three different levels of theory. These calculations largely confirm previous work performed at lower levels of theory,[91−94] which find that an N2-$g_-g_+$ structure is the ground state. Details of the present calculations are provided in Table S1 and Figure S1 of the Supporting Information. For the purposes of the data analysis performed here, the N2-$g_-g_+$ structure is the ground state by several kJ/mol at all three levels of theory performed here. The ordering of the next five conformers differs among all levels including the previous calculations, indicating how subtle the energetic differences are.

**Theory: $M^+$(Cys).** For the $M^+$(Cys) complexes, low-lying and representative higher energy conformations are shown in Figure 3. Table 2 lists the relative energies calculated here with additional geometric parameters detailed in Table S2 of the Supporting Information. We use the nomenclature established previously for $M^+$(Gly),[2,3,95,96] where the notation in brackets describes the metal binding sites for each conformer, followed by a description of the cysteine orientation by a series of four dihedral angles (where c = cis indicates angles <50°, g = gauche for angles between 50° and 135° with + or – indicating its sign, and t = trans for angles >135°). These dihedral angles start with the carboxylic acid hydrogen atom (or analogous proton attached to the $NH_2$ group for zwitterionic structures) to define the ∠HOCC dihedral angle and proceed along the molecule to the terminal hydrogen of the amino acid side chain (∠OCCC, ∠CCCS, and ∠CCSH).

At nearly all levels of theory, the ground state (GS) structure for $Li^+$(Cys), $Na^+$(Cys), and $K^+$(Cys) is the [N,CO,S]-tggg conformer, a tridentate structure in which the metal ion binds to the backbone amino nitrogen, backbone carboxyl oxygen, and the side-chain sulfur. There are two variants of this structure, $tggg_+$ and $tggg_-$, which differ only in whether the SH bond points in the same direction as the carboxylic acid group or the amino group, respectively, Figure 2. The latter structure lies 3−5 kJ/mol higher in energy compared to the former for all three metal cations, perhaps because of a favorable interaction between the SH and carboxylic acid group. For $Rb^+$(Cys), the [N,CO,S]-$tggg_+$ structure is the ground state at the MP2(full) level of theory and is 0.4−5 kJ/mol above the ground state at the two DFT levels of theory, whereas, for $Cs^+$(Cys), calculations indicate this species lies 1 (MP2) or 7−10 (DFT) kJ/mol above the ground state structure. For both $Rb^+$ and $Cs^+$ complexes, the $tggg_-$ variant again lies 3−6 kJ/mol higher than $tggg_+$. There are also [N,CO,S] structures in which the hydroxyl group has rotated 180°, yielding $cggg_+$ and $cggg_-$ conformers.

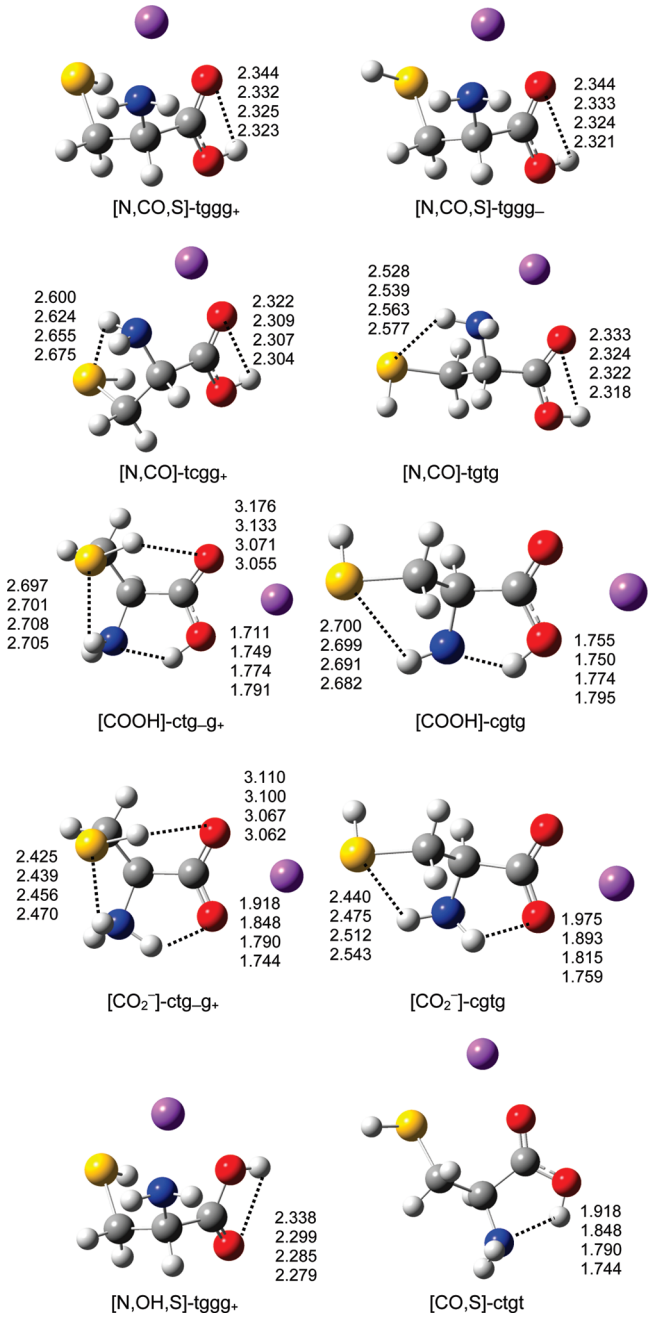


**Figure 2.** $Na^+$(Cys) low-energy structures calculated at the B3LYP/6-311G(d,p) level. Dashes indicate hydrogen bonds with lengths shown in Å for $Li^+$(Cys) (top), $Na^+$(Cys), $K^+$(Cys), and $Rb^+$(Cys) (bottom).

As this breaks the OH···CO hydrogen bond, these structures lie about 25 kJ/mol higher in energy for all metal cations. They were explicitly calculated in the case of $Li^+$(Cys) and found to lie 23−25 kJ/mol above the GS $tggg_+$ conformer.

The next lowest energy type of structure for $Li^+$(Cys) is a series of bidentate [N,CO] structures. There are six variants of this binding motif: $tcgg_+$, tgtg, $tcgg_–$, tctg, tgtt, and tctt, two of which are shown in Figure 2. All six structures are stable for $Na^+$(Cys), whereas the high-lying tctt structure collapses either to tgtt for $Li^+$(Cys) or to tctg for $K^+$(Cys), $Rb^+$(Cys), and $Cs^+$(Cys). For the five variants observed for all five alkali cations, their energies span a range of only 7−10 kJ/mol, consistent with the similar metal cation binding motif among the variants. These [N,CO] structures are found to lie 16−31, 14−26, 9−22, 9−19, and 9−22 kJ/mol above the GS $M^+$(Cys) conformer for $M^+ = Li^+$, $Na^+$, $K^+$, $Rb^+$, and $Cs^+$, respectively. The tctt structure observed for $Na^+$(Cys) lies 13−14 kJ/mol above the $tcgg_+$ variant.

According to the DFT results, the ground state structures for $Rb^+$(Cys) and $Cs^+$(Cys) are bidentate [COOH] geometries in which the metal cation binds to both oxygens of the carboxylic acid group and there is a OH···N hydrogen bond. Again, there are several variants with $ctg_–g_–$ or $ctg_–g_+$ being the lowest in energy for all metal cations, followed by cgtg, cttg, cgtt, and $ctg_+g_–$. The $ctg_–g_–$ or $ctg_–g_+$ variants, which lie within 1 kJ/mol of one another, differ only in whether the SH bond points away from or toward the carboxylic acid group, respectively. The small energy difference is consistent with the long SH···OC hydrogen bond in $ctg_–g_+$, >3 Å, Figure 2. The three lowest energy variants of [COOH] all have a NH···S hydrogen bond, whereas the other three do not. The highest energy variant is $ctg_+g_–$, which lies within 13−17 kJ/mol of the lowest energy [COOH] structure. For $K^+$(Cys), the [COOH]-$ctg_–g_–$ structure lies 3−11 kJ/mol above the [N,CO,S]-$tggg_+$ ground state conformer, whereas the analogous excitation energies for $Li^+$(Cys) and $Na^+$(Cys) are 51−59 and 22−28 kJ/mol, respectively.

Closely related structures are the zwitterionic [$CO_2^–$] complexes in which the metal cation interacts with both oxygens of the carboxylate anion, Figure 2. These zwitterions differ from [COOH] structures primarily in the slight change in the position of the proton shared by the carboxylic and amino groups. The [$CO_2^–$] structures have most of the same variants as the [COOH] structures, except that the cttg structure collapses to cgtt. Here, the $ctg_–g_+$ variant is always the lowest energy structure, presumably because of the stronger hydrogen bond from the SH group to the negatively charged carboxylate. Now, the $ctg_–g_–$ variant lies 3−6 kJ/mol higher in energy, while the $ctg_+g_–$ variant remains highest in energy. The energies of the [$CO_2^–$] structures relative to their [COOH] analogues depend strongly on the metal cation. For $Li^+$ complexes, the zwitterionic structures are preferred by 19−36 kJ/mol, whereas, for $Na^+$(Cys), the difference drops to 5−17 kJ/mol. For the $K^+$(Cys) complexes, the [COOH] and [$CO_2^–$] structures are nearly isoenergetic, lying within 5 kJ/mol of one another for all variants. Generally, the zwitterionic structure of $K^+$(Cys) is preferred by 3−5 kJ/mol, but the low-lying $ctg_–g_–$ variant prefers [COOH] at the B3LYP and MP2(full) levels (but not B3P86) and the high-lying $ctg_+g_–$ variant prefers [COOH] by 3−5 kJ/mol. For $Rb^+$(Cys) and $Cs^+$(Cys), the [COOH] structures are preferred by 1−13 and 8−17 kJ/mol, respectively. Clearly, the higher charge density on the metal cation stabilizes the charge separation in the zwitterionic structures.

At higher energies, there are [CO,S] structures, where the metal cation binds both the carbonyl and the side-chain sulfur. There are three [CO,S] conformations, ctgt, ctcg, and ttgt, for $Li^+$(Cys) and $Na^+$(Cys), but for the heavier metals, the ctcg conformer collapses to a [COOH] $ctg_–g_–$ structure. For $Li^+$, $Na^+$, $K^+$, $Rb^+$, and $Cs^+$ complexes, these conformations are calculated to lie 30−58, 21−45, 11−34, 8−29, and 9−29 kJ/mol, respectively, above the ground state conformers. The three [CO,S] variants span ranges of about 14−21 kJ/mol for all five metal cations. At still higher energies are [N,OH,S] tridentate structures, with $tggg_+$ and $tggg_–$ conformations that are direct analogues of the [N,CO,S] structures except the carboxylic acid group has been rotated by ∼180°. These structures lie 23−34 kJ/mol above their [N,CO,S] analogues for all five metals, with the difference dropping by only 5 kJ/mol in going from $Li^+$(Cys) to $Cs^+$(Cys).

Notably, none of the $M^+$(Cys) complexes exhibit tridentate [COOH,S] or [$CO_2^-$,S] structures in which the metal cation binds to both oxygens of the carboxylic acid (in either charge-solvated or zwitterionic forms) as well as the side-chain sulfur. This is in contrast to previous results for the analogous metal cation complexes of methionine (Met),[9,43] the other sulfur-containing common amino acid. This difference is directly related to the longer side chain in Met, R = $-C_2H_4SCH_3$, compared to R = $-CH_2SH$ for Cys. The longer side chain allows the sulfur to interact effectively with metal cations docked at the carboxylic acid binding site.

Previous calculations of $Na^+$(Cys) conformations have been conducted by Hoyau et al.[20] They located six different conformations at the HF/6-31G(d) level of theory. They also identified the ground state as [N,CO,S] but did not differentiate the two distinct conformations of this binding motif. Likewise, they characterized only one [$CO_2^-$], [N,OH,S], and [N,CO] structure but two [CO,S] variants. The relative energies of the first two of these match the lowest energy structure found here of the same type, whereas lower energy conformations of the [N,CO] and [CO,S] structures are located in the present study, Table 2. In all cases, structural parameters for the metal cation−ligand bond lengths (Table S2 of the Supporting Information) are very similar to the present work. Tsang and co-workers used B3LYP/6-31G(d) theory to characterize only the ground state of the $K^+$(Cys) complex, finding a tridentate [N,CO,S] structure with metal−ligand bond distances similar to those obtained here (Table S2 of the Supporting Information).

**Conversion from 0 to 298 K and Excited Conformers.** Conversion from 0 K bond energies to 298 K bond enthalpies and free energies is accomplished using the rigid rotor/harmonic oscillator approximation with rotational constants and vibrational frequencies calculated at the B3LYP/6-311G(d,p) level. These $\Delta H_{298}$ and $\Delta G_{298}$ values along with the conversion factors and 0 K enthalpies measured here are reported in Table S3 of the Supporting Information. The uncertainties listed are determined by scaling most of the vibrational frequencies by ±10% along with 2-fold variations in the metal−ligand frequencies.

We also calculated the relative $\Delta G_{298}$ values for the four to eight lowest energy structures of each $M^+$(Cys) complex. In general, the relative $\Delta G_{298}$ excitation energies are comparable to the analogous differences in the $\Delta H_0$ values (Table 2), although the free energies of the [N,CO,S] conformers increase by several kJ/mol relative to the other conformers because the tridentate binding restricts the flexibility of the complex more. Using the $\Delta G_{298}$ values to calculate an equilibrium population of conformers shows that the calculated ground state structures for each $M^+$(Cys) system should be dominant in the room temperature ion sources. Excited conformers are calculated to comprise 21−26% of the total for $Li^+$(Cys) with the [N,CO,S]-tggg$_-$ conformer being the only significant contributor. For $Na^+$(Cys), excited conformers comprise 18−32% with the alternate [N,CO,S]-tggg$_-$ conformer contributing 14−19% and [$CO_2^-$] conformers adding only 2−13%. For $K^+$(Cys), the results depend on the level of theory. The [N,CO,S] conformers comprise 23−85% of the calculated population, with [$CO_2^-$] conformers adding 7−46%, [COOH] contributing 7−30%, and [N,CO] conformers contributing 1−2%. For $Rb^+$(Cys), the HW*/6-311+G(2d,2p) results find that the [COOH]-ctg$_-$g$_-$ conformer has the lowest free energy at all three levels of theory, such that it comprises 32−50% of the ion population, with the [COOH]-ctg$_-$g$_+$ and cgtg conformers adding 24−32% and 3−8%, respectively, and the [N,CO,S]-tggg$_+$ contributing another 2−32%. With the Def2TZVP basis set, the percentages change to 22−42, 23−41, 2−10, and 2−43%, respectively.

To investigate the effect of having a different conformer populating the $K^+$(Cys) and $Rb^+$(Cys) cations generated in the ion sources, we analyzed the data using the molecular parameters of several of the low-energy conformers. In all cases, the threshold energies change by less than 2 kJ/mol. The final values listed in Table 1 are an average of the results for the likely conformers, and this effect is included in the uncertainties listed as well.

## Discussion

**Comparison of Theoretical and Experimental Bond Dissociation Energies.** The experimental threshold energies presented in Table 1 are equivalent to the $M^+$−Cys bond dissociation energies at 0 K. For $Li^+$(Cys), the experimental bond energy is taken from the competitive analyses described in a companion paper (DOI 10.1021/jp911222j).[89] For $Na^+$(Cys) and $K^+$(Cys), values obtained from analysis of the FT and ESI data are within experimental error of one another. Therefore, our best experimental bond energies are taken as the weighted average of both values, yielding $D_0(Na^+-Cys) = 1.83 \pm 0.05$ eV = 176.9 ± 5.0 kJ/mol and $D_0(K^+-Cys) = 1.25 \pm 0.03$ eV = 120.7 ± 3.1 kJ/mol. For $Rb^+$(Cys), our best value is taken from analysis of the ESI data. All final values are listed in Table 3.

The theoretical BDEs for the $M^+$(Cys) complexes, where $M^+$ = $Li^+$, $Na^+$, $K^+$, and $Rb^+$, calculated at three levels of theory for all metal cations with and without the core correlation basis set for $Li^+$ are compared to the experimental values in Table 3. We find that all three theoretical methods (B3LYP, B3P86, and MP2) yield BDE values for $M^+$(Cys) that are similar but span ranges of 6−16 kJ/mol. Notably, values for $Rb^+$(Cys) obtained using the Def2TZVP basis set are systematically higher than values obtained using HW*/6-31+G(2d,2p), by an average of 8.4 ± 2.2 kJ/mol. Using the ground state $Rb^+$(Cys) species in all cases ([COOH] for B3LYP and B3P86 and [N,CO,S] for MP2(full)), the HW*/6-311+G(2d,2p) values have a mean absolute deviation (MAD) from the $Rb^+$(Cys) experimental value of 8.1 ± 1.8 kJ/mol (6.3 ± 3.9 kJ/mol if the MP2(full,nocp) value is included), whereas the Def2TZVP values have a MAD of 0.6 ± 0.2 kJ/mol (3.0 ± 4.9 kJ/mol with the MP2(full,nocp) value). There is little ambiguity that the Def2TZVP basis set provides more quantitative agreement between experiment and theory, in agreement with previous results for other $Rb^+$(amino acid) complexes.[10]

Figure 3 shows that the theoretical values are in good agreement with our experimental values especially with regard to the trends. MADs between experiment and various levels of theory range from 2 to 8 kJ/mol (Table 3). When the geometry optimizations and single point energy calculations of the $Li^+$(Cys) systems include core correlation on lithium, the corresponding theoretical BDEs generally increase (partly because counterpoise corrections are not included). Overall, all three levels of theory give comparable agreement with the experimental values. Note that not including kinetic shift effects in the data analysis would shift the theoretical values outside of experimental uncertainties for all metals. Further, if competition with the low-energy decomposition reactions is not included in the analysis of the data for $Li^+$(Cys), the bond energy would be 0.5 eV (49 kJ/mol) higher,[89] such that the agreement with theory would also be much worse.

**Comparison to Literature Bond Energies.** Feng et al.[24] measured the binding free energies ($\Delta G$) for dissociation of

**TABLE 3: Experimental and Theoretical Binding Energies (kJ/mol) at 0 K for $M^+$(Cys)**

| | experiment | | theory[a] | | | | |
|---|---|---|---|---|---|---|---|
| complex | this work | literature | B3LYP (cp) | B3P86 (cp) | MP2(full) (cp) | MP2(full) (nocp) | lit. |
| $Li^+$(Cys) | 255.8 ± 11.9 | 230 ± 14[b] | 260.0 | 251.1 | 245.7 | 258.0 | |
| | | | 263.8[c] | 254.3[c] | | 255.6[c] | |
| $Na^+$(Cys) | 176.9 ± 5.0 | 173 ± 8[d] | 179.6 | 170.2 | 165.8 | 177.5 | 178[e] |
| | | | | | | | 166.2[f] |
| $K^+$(Cys) | 120.7 ± 3.1 | | 120.9 | 117.9 | 119.8 | 126.5 | 123.5[g] |
| $Rb^+$(Cys) | 102.5 ± 2.8 | | 95.6 | 95.2 | 92.3 | 103.4 | |
| | | | 102.1[h] | 101.9[h] | 103.2[h] | 112.9[h] | |
| $Cs^+$(Cys) | | | 83.6 | 83.8 | 81.9 | 89.3 | |
| MAD[i] | | | 3.5 (2.8) | 5.4 (2.0) | 8.1 (4.8) | 2.4 (2.4) | |
| | | | 2.8 (3.6)[c,h] | 2.9 (2.7)[c,h] | 5.7 (5.7)[h] | 4.2 (4.8)[c,h] | |

[a] BDEs for the ground state conformer at the level of theory listed. Geometry optimizations and zero-point energy corrections calculated at the B3LYP/6-311G(d,p) level. Final energies are taken from single point energies calculated at the levels indicated using 6-311+G(2d,2p) basis sets including counterpoise (cp) corrections, except as noted. [b] Value from Feng, Gronert, and Lebrilla,[24] adjusted to $\Delta H_0$ as described in Table S3 of the Supporting Information. [c] Values calculated at the levels indicated using the aug-cc-pVTZ(Li−C) basis set without cp corrections. Geometries and zero-point energies calculated at the MP2(full)/cc-pVDZ(Li−C) level. [d] From Kish et al.,[23] anchored to Ala (179 if anchored to our Gly value, see text). [e] MP2(full)/6-311+G(2d,2p)//MP2/6-31G(d) without cp corrections from Kish et al.,[23] adjusted to 0 K using values in Table S3 of the Supporting Information. [f] MP2(full)/6-311+G(2d,2p)//MP2/6-31G(d) with BSSE corrections from Hoyau et al.,[20] adjusted to 0 K using values in Table S3 of the Supporting Information. [g] B3LYP/6-311+G(3df,2p)//B3LYP/6-31G(d) values with HF/6-31G(d) zero-point energy corrections and no BSSE corrections from Tsang and co-workers.[28] [h] Values calculated using the Def2TZVP basis set. [i] Mean absolute deviations from experiment. Uncertainties in parentheses.

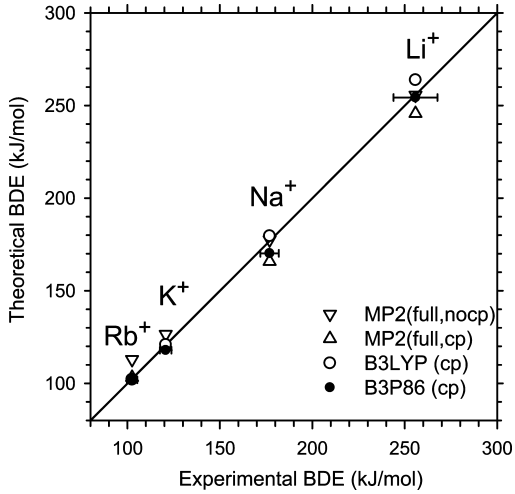


**Figure 3.** Experimental versus theoretical 0 K bond dissociation energies (in eV) calculated at the level of theory shown (R) and taken from Table 3. Values shown for $Li^+$(Cys) are R/aug-cc-pVTZ(Li−C)//MP2(full)/cc-pVDZ(Li−C) results, those for $Na^+$(Cys) and $K^+$(Cys) are R/6-311+G(2d,2p)//B3LYP/6-311G(d,p) results, and those for $Rb^+$(Cys) are R/Def2TZVP//B3LYP/Def2TZVP results. The diagonal line indicates perfect agreement.

$Li^+$(Cys) using the kinetic method with glycine (Gly) and diethoxyethane (DEE) as reference bases. They report an average value of 189 ± 13 kJ/mol at an ion temperature of 373 K. (This temperature is used because the reference values used correspond to this temperature, whereas the estimated temperature in the ion trap was 325 ± 30 K.) A corresponding 0 K enthalpy value of 230 ± 14 kJ/mol is included in Table 3, as deduced here by using $\Delta S_{373}$ = 123 ± 16 J $mol^{-1}$ $K^{-1}$ and ($\Delta H_{373} - \Delta H_0$) = 3.7 ± 1.7 kJ/mol calculated here at the B3LYP/6-311G(d,p) level of theory. This enthalpy is much lower than our experimental and theoretical results, as also recently found for the lithium ion affinities of proline, serine, threonine, and methionine.[5,6,9] There, a number of possible contributions to these discrepancies were discussed, such as a revision in the values used to anchor the absolute values. This would raise the value of Feng et al. by 8 ± 4 kJ/mol, but this still lies 18 kJ/mol below our experimental and theoretical results. Although the absolute values from Feng et al. do not appear reliable, their relative measurements place the lithium cation affinity of Cys above that of Gly by 15 ± 6 kJ/mol. This result qualitatively agrees with our independent measurements, which place the lithium ion affinity of Cys, $D_0(Li^+-Cys)$ = 256 ± 12 kJ/mol, above that of Gly, $D_0(Li^+-Gly)$ = 220 ± 8 kJ/mol,[6] by 36 ± 14 kJ/mol.

Bojesen et al.[18] found that the sodium cation binding affinity for Cys lies between Ala and Val in their relative measurements of the sodium cation affinities of the amino acids, and Kish et al.[23] find it lies above Gly by 14.1 ± 4 kJ/mol. Previously, we have measured $D_0(Na^+-Gly)$ as 164.0 ± 6.0 kJ/mol[2,6] compared to the present value of $D_0(Na^+-Cys)$ = 176.9 ± 5.0 kJ/mol. This yields a difference in sodium cation affinities of 12.9 ± 4.0 kJ/mol at 0 K (where the relative uncertainty in our measurements is smaller than the combined absolute uncertainties because various systematic errors in the measurements cancel). This value translates to a difference at 298 K of 12.2 ± 4.0 kJ/mol, in good agreement with the value of Kish et al. The absolute value reported by Kish et al. for $D_{298}(Na^+-Cys)$ is 175 ± 8 kJ/mol, which translates to $D_0(Na^+-Cys)$ = 173 ± 8 kJ/mol, but this scale is anchored to a value for Ala of 167 ± 8 kJ/mol. If anchored to our value of $D_0(Na^+-Gly)$, their absolute value for $D_0(Na^+-Cys)$ becomes 179 ± 8 kJ/mol. Either the original or reanchored value is in agreement with the value obtained here.

For previous computational results, Hoyau et al. reported that ground state $Na^+$(Cys) has a 298 K binding enthalpy of 167.8 kJ/mol calculated at the MP2(full)/6-311+G(2d,2p)//HF/6-31G(d) level of theory including counterpoise corrections.[20] Adjusting to 0 K (Table S3, Supporting Information) yields a value of 166.2 kJ/mol, which is equivalent to our MP2(full,cp) value of 165.8 kJ/mol (Table 3). The refined theoretical value later given by Kish et al.[23] was 180 ± 4 kJ/mol calculated at the MP2(full)/6-311+G(2d,2p)//MP2/6-31G(d) level without counterpoise corrections. Adjusting to 0 K (Table S3, Supporting Information) gives 178 kJ/mol, which can be favorably compared to our MP2(full,nocp) value of 177.5 kJ/mol. In both cases, the very minor differences (~0.5 kJ/mol) can be attributed to the level of calculation used for the geometry and vibrational frequencies, B3LYP/6-311G(d,p) here. Tsang and co-workers[28] determined a theoretical potassium binding affinity for Cys of 123.5

kJ/mol at 298 K, calculated at the B3LYP/6-311+G(3df,2p)//B3LYP/6-31G(d) level of theory with zero-point energy corrections taken from HF/6-31G(d) frequency calculations. Adjusting to 0 K (Table S3, Supporting Information) gives a value unchanged, in good agreement with our B3LYP value of 120.9 kJ/mol, Table 3, which includes a cp adjustment of 1.4 kJ/mol.

**Side-Chain Substituent Effect.** Metal cations interact with amino acids by electrostatic ion induced−dipole, ion−dipole, and ion−quadrupole forces that lead to solvation of the charge by coordination of the functional groups of the amino acids. Our results for the BDEs required to remove the alkali metal cation from $M^+$(Cys), where $M^+ = Li^+$, $Na^+$, $K^+$, and $Rb^+$ (Table 3), decrease from $Li^+$ to $Rb^+$ because the electrostatic interactions decrease with the increasing bond distances necessitated by the increasing size of the metal cation (radii of 0.70, 0.98, 1.33, and 1.49 Å, respectively).[97] As the metal changes from $Li^+$ to $Na^+$, the BDEs to Cys drop by approximately 85 kJ/mol (∼32%), by another 56 kJ/mol (∼32%) from $Na^+$ to $K^+$, and then by 18 kJ/mol (∼15%) in going to $Rb^+$. The relative BDE decreases are comparable to those measured in our laboratory for $M^+$(Gly), $M^+$(Pro), $M^+$(Ser), $M^+$(Thr), and $M^+$(Met): 26−33% for $Li^+$ to $Na^+$, 23−30% for $Na^+$ to $K^+$, and 10−20% for $K^+$ to $Rb^+$.[2,3,5,10,84,98] When the $M^+$(Cys) BDEs are compared to those of metalated aliphatic amino acids, such as $M^+$(Gly), as well as other bidentate amino acids such as $M^+$(Pro), they are generally larger because the side-chain sulfur group participates in the bonding. Compared to the $M^+$(Gly) systems, the binding energies of $M^+$(Cys) are increased by ∼42 kJ/mol (∼19%) for $Li^+$ and ∼13 kJ/mol (∼8%) for $Na^+$, whereas these two amino acids have similar binding energies to $K^+$, and $Rb^+$ binds Cys more weakly than Gly by ∼6 kJ/mol. These changes are smaller than those for Ser, which has a hydroxyl side chain and always binds more tightly than Gly, by 61 kJ/mol (∼30%) for $Li^+$, 36 kJ/mol (∼20%) for $Na^+$, 24 kJ/mol (∼20%) for $K^+$, and 7 kJ (∼6%) for $Rb^+$. (Note that in all of these comparisons, if the bond energy of $Li^+$(Cys) is uncorrected for competition, the enhancement found would be anomalously large.)

A key difference between the metal cation binding to Ser versus that of Cys is elucidated by examining the structures of $M^+$(Ser) and $M^+$(Cys). In the GS complexes of Ser, theory finds that the metal ion prefers to lie in the HOC plane (∠MCOH dihedral angles of 179−174° for $Li^+$−$Rb^+$), i.e., aligned with the dipole moment of the side-chain hydroxyl group.[6,10] In contrast, the metal ions in the [N,CO,S] Cys complexes have ∠MCSH dihedral angles of 97−110° for $Li^+$−$Rb^+$, indicating that the metal ions interact with one of the two $sp^3$-like lone pair orbitals on sulfur, thereby mediating the interaction of the metal cation with the local dipole. A similar conclusion was found for the structures of the alkali cations with methionine (∠MCS($CH_3$) dihedral angles of 118−128°),[9] the other common amino acid having a sulfur side chain. This orientation is found even though the side chain of Met is longer and more flexible than those of Cys and Ser. Thus, this binding preference is intrinsic to sulfur.

The influence of the local dipole of the side chain is also elucidated by examination of additional trends. Rodgers and Armentrout have previously noted that for several amino acids binding to $Na^+$ and $K^+$ there is a simple linear dependence of the BDEs on the polarizability of the amino acids: Gly (6.6 $Å^3$), Pro (10.3 $Å^3$), Met (14.6 $Å^3$), Phe (18.1 $Å^3$), Tyr (18.8 $Å^3$), and Trp (22.0 $Å^3$).[1,4] (Isotropic molecular polarizabilities were calculated at the PBE0/6-311+G(2d,2p) level of theory using the B3LYP/6-311G(d,p) optimized geometries in the metalated complexes. This level of theory has been shown to provide polarizabilities that are in good agreement with measured values.[99] Values for free ligands are within 2% of the values for the frozen structures from the metalated complexes.) This clearly indicates the importance of ion−induced dipole interactions on the quantitative bond strengths. We recently showed that $Na^+$ and $K^+$ BDEs to Ser (8.6 $Å^3$), Thr (10.5 $Å^3$), Asp (10.45 $Å^3$), Asn (11.2 $Å^3$), Glu (12.2 $Å^3$), and Gln (13.0 $Å^3$) do not fall on the same correlation line but fall on lines parallel with those for Gly, Pro, Met, Phe, Tyr, and Trp.[9] We attributed these differences to the local dipole moment of the side-chain coordinating site. Met, Phe, Tyr, and Trp have small side-chain dipoles, whereas Ser, Thr, Asn, and Gln have larger ones, with Asp and Glu intermediate. In accord with these observations, the contribution of the side-chain dipole of Cys, like that of Met, should be small. Consequently, even though Cys has a larger polarizability (11.2 $Å^3$) than Ser (8.6 $Å^3$), it binds to the alkali cations much less tightly, as quantified above.

The observation that Cys does not follow the correlation with polarizability, e.g., $D_0(K^+-Gly) \approx D_0(K^+-Cys)$ and $D_0(Rb^+-Gly) > D_0(Rb^+-Cys)$, suggests that the presence of the side chain may have inductive or through-space effects that reduce the binding to the carbonyl and amine backbone sites. Indeed, calculations find that, for the potassiated amino acids, the metal−carbonyl bond length increases by 0.07 Å in going from $K^+$(Gly) [N,CO] to $K^+$(Cys) [N,CO,S], whereas the metal−nitrogen bond decreases by 0.02 Å. Likewise, in the analogous rubidiated complexes, the Rb−CO bond length increases by 0.06 (0.07 using the Def2TZVP basis set) Å and the Rb−N bond length decreases by 0.09 (0.04) Å. However, the DFT ground state structures for the rubidiated systems are $Rb^+$(Gly) [CO] and $Rb^+$(Cys) [COOH] $ctg_-g_-$, in which the Rb−CO bond length increases by 0.09 (0.09) Å in going from $Rb^+$(Gly) [CO] to $Rb^+$(Cys) [COOH] (increases of 0.12 (0.13) Å for the [COOH] $ctg_-g_+$ conformer). Indeed, the fact that the rubidium cation binds only to the carbonyl of glycine but to both oxygens in cysteine illustrates the effect of the side chain as well. The OH···NH···S hydrogen bonds in $Rb^+$(Cys) [COOH], Figure 2, move electron density toward the hydroxyl group, thus making the hydroxyl group a better electron donor. However, this also means that the metal cation no longer aligns along the carbonyl bond, the most favorable binding site for a carbonyl.[2,3] A SH···OC hydrogen bond in the $ctg_-g_+$ conformer probably explains why the $Rb^+$−OC bond lengths are 0.02−0.03 Å longer in this [COOH] conformer than in the $ctg_-g_-$ variant (Table S2, Supporting Information).

## Conclusion

The kinetic energy dependences of the collision-induced dissociation (CID) of $M^+$(Cys), where $M^+ = Li^+$, $Na^+$, $K^+$, and $Rb^+$, are examined in a guided ion beam tandem mass spectrometer. The primary cross section in all cases is the loss of an amino acid from the complex, although deamination is also found for $Li^+$(Cys).[89] The apparent threshold for removing Cys follows the order of $Li^+$(Cys) > $Na^+$(Cys) > $K^+$(Cys) > $Rb^+$(Cys), as expected for the variations in charge density on the metal ion. BDEs at 0 K for losing Cys from the complexes, Table 3, are obtained by detailed modeling of the experimental cross sections, including competition with the alternate low-energy decomposition pathways found for $Li^+$(Cys).[89]

Three different levels of quantum chemical calculations including zero-point energy corrections and counterpoise corrections for basis set superposition errors were performed for all $M^+$(Cys) complexes. For $Li^+$(Cys), calculations employing

basis sets with core correlation on Li (cc-pCVTZ) and aug-cc-pVTZ for other atoms were performed, and for $Rb^+$(Cys), the Def2TZVP basis set was also used. The calculated BDEs for losing Cys from the $M^+$(Cys) complexes agree well with our experimental values, Table 3 and Figure 3. Notably, the HW* basis set for Rb underestimates the BDEs by about 8 kJ/mol, whereas the Def2TZVP basis set yields theoretical values in good agreement with experiment, in good agreement with previous results for other $Rb^+$(amino acid) complexes.[10]

The experimental 0 K BDEs of $M^+$(Cys) are much smaller than those of the analogous $M^+$(Ser) complexes even though the complexes are both tridentate for most metal cations and the polarizability of Cys is larger than that of Ser. This is attributed to differences in the local dipole moments of the side chain functionalities, which leads to substantial changes in the orientation of the side chain. Further, the experimental 0 K BDEs for $M^+$(Cys) compared to $M^+$(Gly) are larger for the smaller cations, $Li^+$ and $Na^+$, but nearly the same for $K^+$, and weaker for $Rb^+$. This is attributed to inductive effects associated with hydrogen bonding of the side chain.

**Acknowledgment.** This work is supported by the National Science Foundation, CHE-0748790 and CHE-0649039. A grant of computer time from the Center for High Performance Computing at the University of Utah is gratefully acknowledged. Amy Gabriel and Dr. Robert M. Moision are thanked for taking some of the flow tube data.

**Supporting Information Available:** Description of structures of neutral cysteine along with a figure and table of relative energies. Table of geometrical parameters of the various $M^+$(Cys) conformers. Table of 0−298 K conversions of bond energies and enthalpies. This material is available free of charge via the Internet at http://pubs.acs.org.

## References and Notes

(1) Rodgers, M. T.; Armentrout, P. B. *Acc. Chem. Res.* **2004**, *37*, 989–998.
(2) Moision, R. M.; Armentrout, P. B. *J. Phys. Chem. A* **2002**, *106*, 10350–10362.
(3) Moision, R. M.; Armentrout, P. B. *Phys. Chem. Chem. Phys.* **2004**, *6*, 2588–2599.
(4) Ruan, C.; Rodgers, M. T. *J. Am. Chem. Soc.* **2004**, *126*, 14600–14610.
(5) Moision, R. M.; Armentrout, P. B. *J. Phys. Chem. A* **2006**, *110*, 3933.
(6) Ye, S. J.; Clark, A. A.; Armentrout, P. B. *J. Phys. Chem. B* **2008**, *112*, 10291–10302.
(7) Heaton, A. L.; Moision, R. M.; Armentrout, P. B. *J. Phys. Chem. A* **2008**, *112*, 3319–3327.
(8) Heaton, A. L.; Armentrout, P. B. *J. Phys. Chem. B* **2008**, *112*, 12056–12065.
(9) Armentrout, P. B.; Gabriel, A.; Moision, R. M. *Int. J. Mass Spectrom.* **2009**, *283*, 56–68.
(10) Bowman, V. N.; Heaton, A. L.; Armentrout, P. B. *J. Phys. Chem. B* **2010**, in press. DOI: 10.1021/jp101264m.
(11) Meinnel, T.; Blanquet, S.; Dardel, F. *J. Mol. Biol.* **1996**, *262*, 375–386.
(12) Nemirovskiy, O. V.; Gross, M. L. *J. Am. Soc. Mass Spectrom.* **1998**, *9*, 1285–1292.
(13) Endoa, I.; Nojiria, M.; Tsujimuraa, M.; Nakasakoc, M.; Nagashima, S.; Yohda, M.; Odaka, M. *J. Inorg. Biochem.* **2001**, *83*, 247–253.
(14) Miyanaga, A.; Fushinobu, S.; Ito, K.; Wakagi, T. *Biochem. Biophys. Res. Commun.* **2001**, *288*, 1169–1174.
(15) Mathe, C.; Mattioli, T. A.; Horner, O.; Lombard, M.; Latour, J.-M.; Fontecave, M.; Niviere, V. *J. Am. Chem. Soc.* **2002**, *124*, 4966–4967.
(16) Shindo, M.; Irie, K.; Fukudaa, H.; Ohigashib, H. *Bioorg. Med. Chem.* **2003**, *11*, 5075–5082.
(17) Giles, N. M.; Watts, A. B.; Giles, G. I.; Fry, F. H.; Littlechild, J. A.; Jacob, C. *Chem. Biol.* **2003**, *10*, 677–693.
(18) Bojesen, G.; Breindahl, T.; Andersen, U. N. *Org. Mass Spectrom.* **1993**, *28*, 1448–1452.
(19) Andersen, U. N.; Bojesen, G. *J. Chem. Soc., Perkins Trans. 2* **1997**, 323–326.
(20) Hoyau, S.; Norrman, K.; McMahon, T. B.; Ohanessian, G. *J. Am. Chem. Soc.* **1999**, *121*, 8864–8875.
(21) Cerda, B. A.; Wesdemiotis, C. *Analyst* **2000**, *125*, 657–660.
(22) Ryzhov, V.; Dunbar, R. C.; Cerda, B. A.; Wesdemiotis, C. *J. Am. Soc. Mass Spectrom.* **2000**, *11*, 1037–1046.
(23) Kish, M. M.; Ohanessian, G.; Wesdemiotis, C. *Int. J. Mass Spectrom.* **2003**, *227*, 509–524.
(24) Feng, W. Y.; Gronert, S.; Lebrilla, C. B. *J. Phys. Chem. A* **2003**, *107*, 405–410.
(25) Kapota, C.; Lemaire, J.; Maitre, P.; Ohanessian, G. *J. Am. Chem. Soc.* **2004**, *126*, 1836–1842.
(26) Cooks, R. G.; Wong, P. H. *Acc. Chem. Res.* **1998**, *31*, 379–386.
(27) Cooks, R. G.; Koskinen, J. T.; Thomas, P. D. *J. Mass Spectrom.* **1999**, *34*, 85–92.
(28) Lau, J. K.-C.; Wong, C. H. S.; Ng, P. S.; Siu, F. M.; Ma, N. L.; Tsang, C. W. *Chem.—Eur. J.* **2003**, *9*, 3383–3396.
(29) Cerda, B. A.; Wesdemiotis, C. *J. Am. Chem. Soc.* **1995**, *117*, 9734–9739.
(30) Lee, V. W.-M.; Li, H.; Lau, T.-C.; Guevremont, R.; Siu, K. W. M. *J. Am. Soc. Mass Spectrom.* **1998**, *9*, 760–766.
(31) Jensen, F. *J. Am. Chem. Soc.* **1992**, *114*, 9533–9537.
(32) Hoyau, S.; Ohanessian, G. *Chem.—Eur. J.* **1998**, *4*, 1561–1569.
(33) Marino, T.; Russo, N.; Toscano, M. *Inorg. Chem.* **2001**, *40*, 6439–6443.
(34) Marino, T.; Russo, N.; Toscano, M. *J. Phys. Chem. B* **2003**, *107*, 2588–2594.
(35) Marino, T.; Russo, N.; Toscano, M. *J. Inorg. Biochem.* **2000**, *79*, 179–185.
(36) Polfer, N. C.; Oomens, J.; Dunbar, R. C. *Phys. Chem. Chem. Phys.* **2006**, *8*, 2744–2751.
(37) Forbes, M. W.; Bush, M. F.; Polfer, N. C.; Oomens, J.; Dunbar, R. C.; Williams, E. R.; Jockusch, R. A. *J. Phys. Chem. A* **2007**, *111*, 11759–11770.
(38) Armentrout, P. B.; Rodgers, M. T.; Oomens, J.; Steill, J. D. *J. Phys. Chem. A* **2008**, *112*, 2248–2257.
(39) Rodgers, M. T.; Armentrout, P. B.; Oomens, J.; Steill, J. D. *J. Phys. Chem. A* **2008**, *112*, 2258–2267.
(40) O'Brien, J. T.; Prell, J. S.; Steill, J. D.; Oomens, J.; Williams, E. R. *J. Phys. Chem. A* **2008**, *112*, 10823–10830.
(41) Klassen, J. S.; Anderson, S. G.; Blades, A. T.; Kebarle, P. *J. Phys. Chem.* **1996**, *100*, 14218–14227.
(42) Heaton, A. L.; Bowman, V. N.; Oomens, J.; Steill, J. D.; Armentrout, P. B. *J. Phys. Chem. A* **2009**, *113*, 5519–5530.
(43) Carl, D. R.; Cooper, T. E.; Oomens, J.; Steill, J. D.; Armentrout, P. B. *Phys. Chem. Chem. Phys*., DOI: 10.1039/b926429a.
(44) Stennett, E. M. S.; Oomens, J.; Steill, J. D.; Rodgers, M. T.; Armentrout, P. B. Work in progress.
(45) Ye, S. J.; Armentrout, P. B. *J. Phys. Chem. B* **2008**, *112*, 10303–10313.
(46) Ervin, K. M.; Armentrout, P. B. *J. Chem. Phys.* **1985**, *83*, 166–189.
(47) Muntean, F.; Armentrout, P. B. *J. Chem. Phys.* **2001**, *115*, 1213–1228.
(48) Schultz, R. H.; Crellin, K. C.; Armentrout, P. B. *J. Am. Chem. Soc.* **1991**, *113*, 8590–8601.
(49) Fenn, J. B.; Mann, M.; Meng, C. K.; Wong, S. F.; Whitehouse, C. M. *Mass Spectrom. Rev.* **1990**, *9*, 37–70.
(50) Moision, R. M.; Armentrout, P. B. *J. Am. Soc. Mass Spectrom.* **2007**, *18*, 1124–1134.
(51) Fisher, E. R.; Armentrout, P. B. *J. Chem. Phys.* **1991**, *94*, 1150–1157.
(52) Fisher, E. R.; Kickel, B. L.; Armentrout, P. B. *J. Chem. Phys.* **1992**, *97*, 4859–4870.
(53) Rodgers, M. T.; Armentrout, P. B. *J. Phys. Chem. A* **1997**, *101*, 1238–1249.
(54) Rodgers, M. T.; Armentrout, P. B. *Int. J. Mass Spectrom.* **1999**, *185/186/187*, 359–380.
(55) Rodgers, M. T.; Armentrout, P. B. *J. Phys. Chem. A* **1999**, *103*, 4955–4963.
(56) Kim, T.; Tolmachev, A. V.; Harkewicz, R.; Prior, D. C.; Anderson, G.; Udseth, H. R.; Smith, R. D. *Anal. Chem.* **2000**, *72*, 2247–2255.
(57) Ye, S. J.; Armentrout, P. B. *J. Phys. Chem. A* **2008**, *112*, 3587–3596.
(58) Gerlich, D. *Adv. Chem. Phys.* **1992**, *82*, 1–176.
(59) Hales, D. A.; Lian, L.; Armentrout, P. B. *Int. J. Mass Spectrom. Ion Processes* **1990**, *102*, 269–301.
(60) Daly, N. R. *Rev. Sci. Instrum.* **1960**, *31*, 264–267.
(61) Beyer, T. S.; Swinehart, D. F. *Commun. Assoc. Comput. Mach.* **1973**, *16*, 379.
(62) Stein, S. E.; Rabinovich, B. S. *J. Chem. Phys.* **1973**, *58*, 2438–2445.

(63) Stein, S. E.; Rabinovich, B. S. *Chem. Phys. Lett.* **1977**, *49*, 183–188.
(64) Gilbert, R. G.; Smith, S. C. *Theory of Unimolecular and Recombination Reactions*; Blackwell Scientific: London, 1990.
(65) Truhlar, D. G.; Garrett, B. C.; Klippenstein, S. J. *J. Phys. Chem.* **1996**, *100*, 12771–12800.
(66) Holbrook, K. A.; Pilling, M. J.; Robertson, S. H. *Unimolecular Reactions*, 2nd ed.; Wiley: New York, 1996.
(67) Rodgers, M. T.; Ervin, K. M.; Armentrout, P. B. *J. Chem. Phys.* **1997**, *106*, 4499–4508.
(68) Rodgers, M. T.; Armentrout, P. B. *J. Chem. Phys.* **1998**, *109*, 1787–1800.
(69) Meyer, F.; Khan, F. A.; Armentrout, P. B. *J. Am. Chem. Soc.* **1995**, *117*, 9740–9748.
(70) Koizumi, H.; Armentrout, P. B. *J. Am. Soc. Mass Spectrom.* **2001**, *12*, 480–489.
(71) Ye, S. J.; Moision, R. M.; Armentrout, P. B. *Int. J. Mass Spectrom.* **2006**, *253*, 288–304.
(72) More, M. B.; Ray, D.; Armentrout, P. B. *J. Phys. Chem. A* **1997**, *101*, 831–839.
(73) More, M. B.; Ray, D.; Armentrout, P. B. *J. Phys. Chem. A* **1997**, *101*, 4254–4262.
(74) More, M. B.; Ray, D.; Armentrout, P. B. *J. Phys. Chem. A* **1997**, *101*, 7007–7017.
(75) Waage, E. V.; Rabinovitch, B. S. *Chem. Rev.* **1970**, *70*, 377–387.
(76) Armentrout, P. B.; Simons, J. *J. Am. Chem. Soc.* **1992**, *114*, 8627–8633.
(77) McLean, A. D.; Chandler, G. S. *J. Chem. Phys.* **1980**, *72*, 5639.
(78) Krishnan, R.; Binkley, J. S.; Seeger, R.; Pople, J. A. *J. Chem. Phys.* **1980**, *72*, 650.
(79) Foresman, J. B.; Frisch, A. E. *Exploring Chemistry with Electronic Structure Methods*, 2nd ed.; Gaussian, Inc.: Pittsburgh, PA, 1996.
(80) Boys, S. F.; Bernardi, R. *Mol. Phys.* **1970**, *19*, 553–566.
(81) van Duijneveldt, F. B.; van Duijneveldt de Rijdt, J. G. C. M.; van Lenthe, J. H. *Chem. Rev.* **1994**, *94*, 1873–1885.
(82) Ye, S. J.; Moision, R. M.; Armentrout, P. B. *Int. J. Mass Spectrom.* **2005**, *240*, 233–248.
(83) Armentrout, P. B.; Rodgers, M. T. *J. Phys. Chem. A* **2000**, *104*, 2238–2247.
(84) Rodgers, M. T.; Armentrout, P. B. *Int. J. Mass Spectrom.* **2007**, *267*, 167–182.
(85) Hay, P. J.; Wadt, W. R. *J. Chem. Phys.* **1985**, *82*, 299–310.
(86) Glendening, E. D.; Feller, D.; Thompson, M. A. *J. Am. Chem. Soc.* **1994**, *116*, 10657–10669.
(87) Weigend, F.; Ahlrichs, R. *Phys. Chem. Chem. Phys.* **2005**, *7*, 3297.
(88) Leininger, T.; Nicklass, A.; Kuechle, W.; Stoll, H.; Dolg, M.; Bergner, A. *Chem. Phys. Lett.* **1996**, *255*, 274–280.
(89) Armentrout, P. B.; Ye, S. J.; Gabriel, A.; Moision, R. M. *J. Phys. Chem. B*. DOI: 10.1021/jp911222j.
(90) Rodgers, M. T.; Armentrout, P. B. *Mass Spectrom. Rev.* **2000**, *19*, 215–247.
(91) Gronert, S.; O'Hair, R. A. J. *J. Am. Chem. Soc.* **1995**, *117*, 2071–2081.
(92) Tian, Z.; Pawlow, A.; Poutsma, J. C.; Kass, S. R. *J. Am. Chem. Soc.* **2007**, *129*, 5403–5407.
(93) Noguera, M.; Rodriguez-Santiago, L.; Sodupe, M.; Bertran, J. *THEOCHEM* **2001**, *537*, 307–318.
(94) Spezia, R.; Tournois, G.; Cartailler, T.; Tortajada, J.; Jeanvoine, Y. *J. Phys. Chem. A* **2006**, *110*, 9727–9735.
(95) Rodriguez-Santiago, L.; Sodupe, M.; Tortajada, J. *J. Phys. Chem. A* **2001**, *105*, 5340–5347.
(96) Bertran, J.; Rodriguez-Santiago, L.; Sodupe, M. *J. Phys. Chem. B* **1999**, *103*, 2310–2317.
(97) Wilson, R. G.; Brewer, G. R. *Ion Beams with Applications to Ion Implantation*; Wiley: New York, 1973.
(98) Moision, R. M.; Armentrout, P. B. Unpublished work.
(99) Smith, S. M.; Markevitch, A. N.; Romanor, D. A.; Li, X.; Levis, R. J.; Schlegel, H. B. *J. Phys. Chem. A* **2004**, *108*, 11063–11072.

JP911219U